Experimental and Numerical Investigation of Bond Performance of RC tension members

Alinda Dey[1,*], Domas Valiukas[2], Aleksandr Sokolov[3], Ronaldas Jakubovskis[4], Gintaris Kaklauskas[5]

1. PhD student, Department of Reinforced Concrete Structures and Geotechnics, Vilnius Tech, Vilnius, Lithuania
2. PhD student, Department of Reinforced Concrete Structures and Geotechnics, Vilnius Tech, Vilnius, Lithuania
3. PhD, Laboratory of Innovative Building Structures, Vilnius Tech, Vilnius, Lithuania
4. PhD, Department of Reinforced Concrete Structures and Geotechnics, Vilnius Tech, Vilnius, Lithuania
5. Professor, Department of Reinforced Concrete and Geotechnics, Vilnius Tech, Vilnius, Lithuania

[*]Corresponding author email: alinda.dey@vilniustech.lt

Abstract

The bond behaviour between concrete and reinforcement is the root aspect of the reinforced concrete structural performance, both regarding safety and serviceability. To perceive the precise bond behaviour at the concrete-reinforcement interface, a glimpse from the reinforcement core (embedded inside the concrete) is essential. In this article, the bond performance of the deformed bar was investigated both experimentally and numerically. A double pull-out test was performed with tensor strain gauges installed within the modified reinforcement bar. With this reference, two alternative approaches were investigated by finite element (FE) analysis. At first, a plain reinforcement with varied bonding conditions at the specific interval was modelled in three dimensions (*Model-1*). Secondly, a three-dimensional model with a simplified rib geometry conforming to a predefined bonding index of standard ribbed steel reinforcement was considered as *Model 2*. Particular focus has been given to the rib geometry as one of the dominating factors to comply with FE models. Moreover, the present article comprises comparative study between two developed FE models and each approach's efficiency is validated with the experimental bond stress along with the bond-slip relation.

Keywords: *bond-slip relationship, bond stress, double pull-out test, finite element analysis, reinforced concrete.*

1. Introduction

The worldwide demand and adoption of Reinforced Concrete (RC) made it the most successful structural material. However, it is a composite material, appropriate force transfer between the reinforcing bars and surrounding concrete is necessary in order to ensure structural stability and continuity. This force transfer takes place through the interaction between reinforcement and concrete (referred to as bond). The latter being the central issue, which governs both the performance and the behaviour of all RC structures particularly when the serviceability is concerned.

The bond between concrete and steel is the combination of frictional resistance, chemical adhesion and mechanical interlock. Frictional resistance occurs due to the surface roughness of the reinforcing bar as well as the shrinkage in the concrete. Hydration of cement and the presence of ribs on the bar surface are responsible for chemical adhesion and mechanical interlock, respectively (Dey et al., 2021; Sulaiman et al., 2017). The stress, which helps to hold the bond between concrete and reinforcement, is referred to as bond stress. About 20% of the total bonding stress is due to both the adhesion and frictional resistance between two different materials. The rest of bond stresses are transferred by means of mechanical interlock between the profiled ribs of reinforcement bars and concrete. At the contact surface of reinforcement rib, the concrete undergoes complex mechanical actions, including local bearing, crushing, compression, shearing, which lead to a specific pattern of cracking, reported by authors on their studies (Borosnyói & Snóbli, 2010; Goto, 1971).

The bond between the reinforcing bar and the concrete can be further categorized into flexural bond and anchorage bond. The former prevails during the change in bending moment along the length of the member, whereas the anchorage bond evolves along the development length, responsible for the transfer of forces from the reinforcing bar to the surrounding concrete (Siempu & Pancharathi, 2018). Flexural bond is usually obtained from full-scale beam test and the anchorage bond from the direct pull-out test (Sulaiman et al., 2017). The latter is more common and mostly used for its simplicity and ease in execution. Such tests offer average bond stress distribution through the anchorage length in terms of relative displacement (slip) between reinforcing bar and concrete.

In an alternative way, the glimpse of concrete-reinforcement interaction (bond-slip behaviour) can be obtained from the experimental strain data of the reinforcement bar embedded in the concrete. Installation of electrical strain gauges inside the reinforcement ensures accurate strain measurement in the double pull-out test (Dey et al., 2020). This test is slightly intricate, but it imparts a realistic picture of force transfer mechanism between the reinforcing steel and concrete, which can lead to an explicit and reliable study of the bond mechanics and bond-slip models (Kaklauskas et al., 2019).

Numerous authors investigated the bond phenomenon in the past, but due to its inherently complex nature it is still not entirely predictable (Balázs, 2007; Gambarova, 2012). The prediction becomes more difficult when the bond damage in the vicinity of a crack comes into the picture. Due to the constant physical and mechanical actions, some part of the bonding zone deteriorates, which further has a significant influence on the deformation of RC structures. Bond deterioration remarkably reduces the stiffness of the RC members (Bernardi et al., 2014) and has the ability to change the crack formation pattern i.e. crack width and crack spacing (Kaklauskas, 2017). Focusing on the damage in concrete, particularly at the close vicinity of the ribs, numerical modelling emerged as an effective tool of analysis. A few experiments based on finite element modelling have been conducted to understand the bond mechanism (Jendele & Cervenka, 2006; Ruiz et al., 2007; Santos & Abel, 2015). However, these studies were not much emphasized the bond deterioration pattern. Later on modified rib-scale models were investigated with two-dimensional representation (Daoud et al., 2013; Salem & Maekawa, 2004). It is seen that two-dimensional models are unable to consider the circumferential tensile stresses, which are responsible for splitting cracks in concrete and results certain reduction in the bond stress value (Kanazawa et al., 2017). Circumferential stress was later considered in three-dimensional approaches of finite element modelling. Such modelling was reported to be extremely delicate and time-consuming but accurate at the same time, for their fine and precise finite element mesh, particularly around the rebar (Jakubovskis & Kaklauskas, 2019; Shang et al., 2011).

In this paper, two different finite element models were developed mainly for the comparative study in terms of the bond behaviour in the RC prisms under tensile loads. The result can be effectively utilized for future parametric analysis. Alongside, a test of a reinforced concrete prism subjected to the tension was carried out to investigate the adequacy of the numerical models. The first numerical approach seemed to have a better correlation with test results at lower loading stages, whereas the model with simplified rib geometry manifested better soundness at serviceability loads, thus considered to be more precise, when qualitatively predicting bond stress distribution along the reinforcing bars. The latter model can be considered as a good instrument for splitting crack and lateral crack quantitative analysis, as well as for the damaged concrete zone in the vicinity of the reinforcement.

2. Experimental Program

2.1. Specimen

This experimental campaign was performed at the laboratory of Vilnius Tech University (Vilnius Gediminas Technical University). It aimed at investigating the interaction between reinforcement and the surrounding concrete in the RC tensile member (tie) by the double pull-out test. Strain recording from the embedded reinforcement is the basis of this study. The specimen (RC prism) used in this test was of 150mm x 150mm cross-section, 210mm length and was reinforced with a single bar of 20mm diameter. In order to avoid the cracks, the specimen length (210 mm) was taken smaller than the mean crack spacing s_{rm} = 250mm (Kaklauskas et al., 2017).The specimen is graphically illustrated in Figure 1.

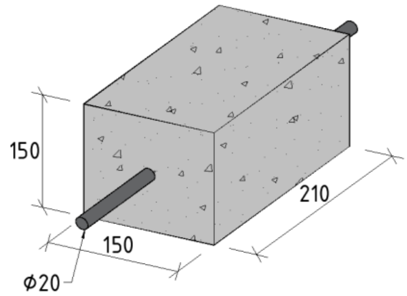

Figure 1. Illustration of the RC tie to clarify its dimensional characteristics

The strain gauge installation procedure inside the rebar itself was delicate and time consuming. Two longitudinal halves were cut from two different Ø-20 mm reinforcement. Then small longitudinal groove of 10mm x 2mm was made on each half of the reinforcement through its entire length. 13 strain gauges were placed 20 mm apart inside the grooves including the necessary soldering and wiring. Post installation, the two halves were attached by clamping with epoxy glue and the single modified steel bar was prepared. It is worth mentioning that epoxy glue was only provided at the interface between the two parts of the reinforcement and it does not contribute to the stiffness of the rebar as it is very elastic. The cross-section and the section along the longitudinal axis are illustrated in Figure 2. It is clearly noticeable that the extreme strain gauges were kept outside the concrete in order to obtain the actual reinforcement strain without concrete intervention.

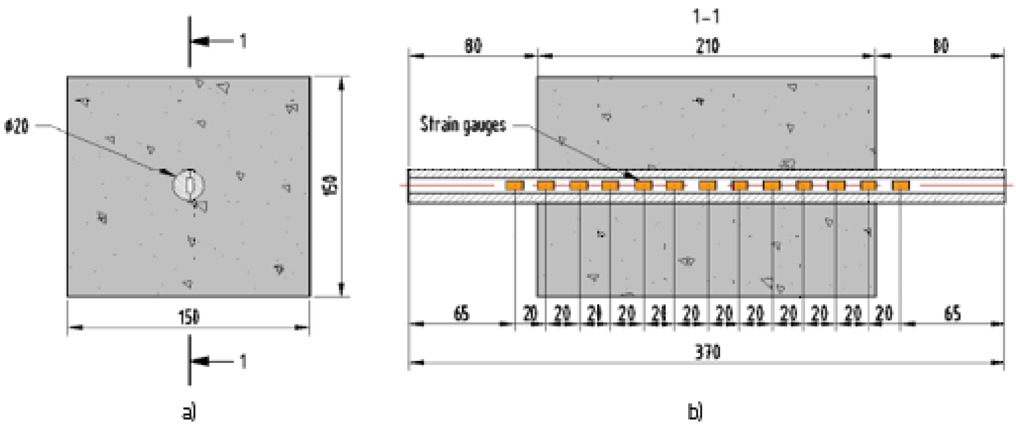

Figure 2. Installation and spacing of strain gauges a) cross-sectional view and b) longitudinal layout

2.2. Material properties

The concrete mix was prepared by the combination of Ordinary Portland Cement, water, natural pit sand of 0/4 mm grade and gravel of 5/8 mm grade proportionally. A specific amount of concrete plasticizer was used for workability purpose. The concrete strength was obtained through the conventional cylinder (150 mm diameter and 300 mm height) test after 28 days of proper curing. Uniaxial test of bare rebar (S500 grade) was also performed to determine its yielding strength and modulus of elasticity. Physical specifications of the specimen and its mechanical properties are demonstrated in Table 1.

Table 1. Physical and Mechanical Characteristics of the specimen

Physical Specification		Mechanical Properties		
HxBxL(mm)	150x150x210	Concrete	f_{cm} (MPa)	44.8

Bar diameter (mm)	20		Ec (MPa)	33787
Groove dimension (mm)	2(2x10)	Steel	fy (MPa)	486
As (mm^2)	270.8		Es (MPa)	201734

2.3. Test setup

A double pull out test was performed on the mentioned specimen using a Universal Testing Machine (UTM). The load was applied in a monotonic manner by using displacement controlled method. The strain data was sampled every 1kN increase in the applied load, until the maximum 90kN.

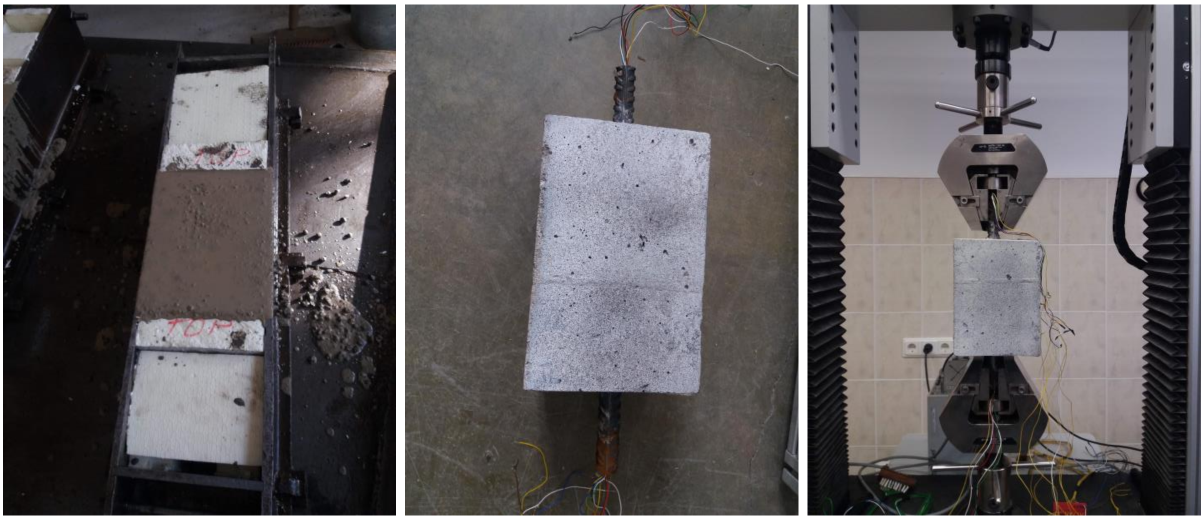

Figure 3. Photographical report of the experimental test in laboratory

3. Numerical Modelling

Two types of finite element models were developed using computer software package ATENA (Cervenka et al., 2007) and underwent through non-linear analysis. Firstly, *Model-1* consists of 3D tetrahedral finite elements with plain reinforcement. Different bonding conditions on cylindrical surface of rebar was applied to simulate mechanical behaviour of reinforcement ribs. In the other words, mechanical ribs were replaced with distinguished surface zones of much higher bonding properties, this provides the advantage of short computational time during non-linear analysis. The second one, *Model-2* takes into account the actual geometry of reinforcement rib, though in a simplified manner. In the experimental approach, part of steel reinforcement was milled out, in order to accommodate the strain gauges, while in FE approaches, the full cross sectional area of rebar was modelled. Now to neutralize the discrepancy, the external load was artificially increased in a measured way during the numerical analysis. More detailed model descriptions are provided in the following sub-sections.

3.1. Numerical 3D model 1

The analysis of Finite Element (FE) *Model-1* is graphically represented in Figure 4. One-eighth of the real-life specimen was considered, thus suitable boundary conditions were applied on three faces of model. Geometrical non-linear analysis with sparse-iterative solver was chosen. Isoparametric tetrahedral finite elements with 10 nodes were used. Concrete was modelled as 3D nonlinear cementitious material (given as default material in *ATENA*) with the following mechanical properties: tensile strength $f_t = 3.374$ MPa, compressive strength of cylinder $f_{ck} = 44.8$ MPa, modulus of elasticity $E_c = 37630$ MPa, specific fracture energy $G_f = 84.3$ N/m (fib Model Code, 2013). Reinforcement was modelled as linear elastic material with the following mechanical properties obtained by testing: modulus of elasticity $E_s = 201734$ MPa, yield strength $f_y = 486$ MPa. In this *Model-1* the geometry of reinforcement is replaced by array of cylinders with different bonding characteristics (Figure 4). "Strong" bond area represents the ribs of reinforcement, while the "normal" bond conditions represents area between the ribs. Main variable parameters affecting bonding, and therefore used for FE model calibration are as follow: f_t – tensile strength of the bond, c – adhesion strength of bond, K_{nn} and K_{tt} are the normal and tangential stiffness of bond respectively and φ is the friction coefficient on the interface of two materials. This is worth mentioning that, numerical values for different parameters affecting the bond behaviour (mentioned previously) were obtained mainly by testing – i.e. parameters had been changed until satisfactory compliance with experimental steel strain curve was achieved. Study has shown, that the most critical parameters are tensile strength of the bond, normal and tangential stiffness of bond.

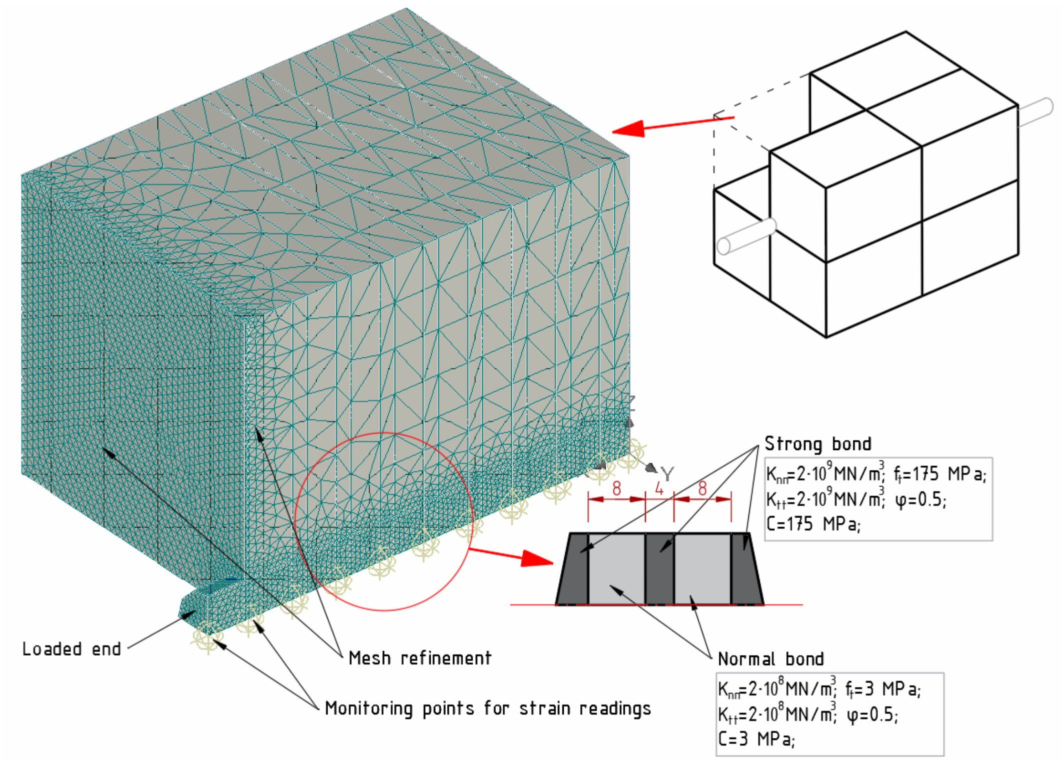

Figure 4. FE Model-1 with assumed bond characteristics

Figure 5 represents the concrete strains, where the colour filter is set in such a manner that strains up to cracking ($\varepsilon_{cr} = 8.97 \cdot 10^{-5}$) are displayed in grey colour and strains more than 0.003 are shown in light blue. As predicted, higher deformation values are observed at the zones with "strong" bond options. Though the model is simple and demonstrated a good congruence with experimental model at low to mid-level loads. However, it also has some serious drawbacks. Most importantly, sudden failure of bonding has been observed, probably because of the surrounding circumferential concrete ring, which did not contribute to any radial pressure. For the same reason this *Model-1* was unable to capture formation of splitting cracks. Keeping this fact in mind, a more complicated three-dimensional model is adopted with simplified rib geometry in the chapter below.

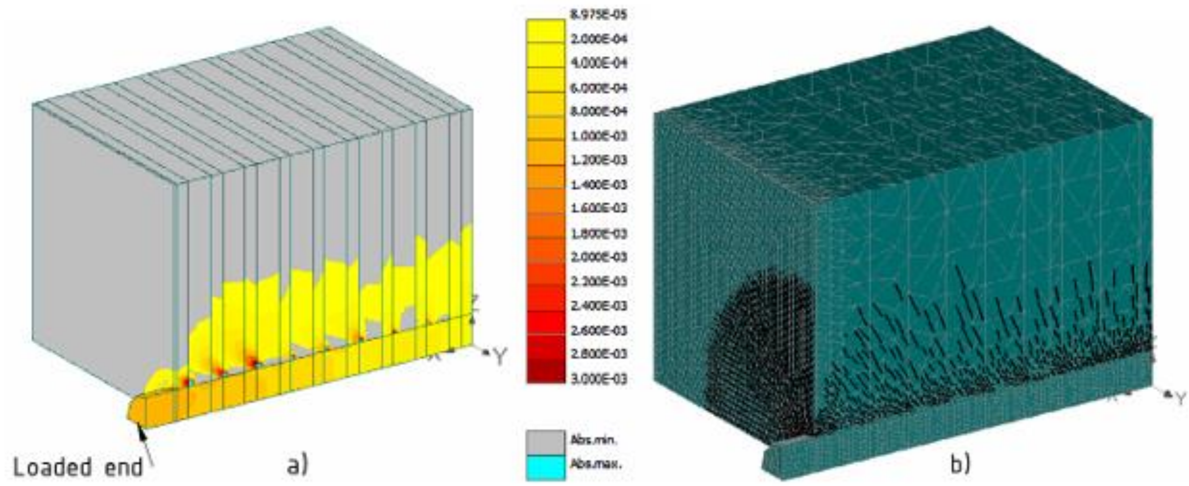

Figure 5. FE Model-1 (a) longitudinal concrete strain profile and (b) failure mechanics

3.2. Numerical 3D model 2

It is earlier discussed that the most important stress transmission path from rebar to concrete is secured through the mechanical bearing of reinforcement ribs (Lutz & Gergely, 1967). This three-dimensional *Model-2* (Figure 6) implements the complex shape of nominal reinforcement rib to a simplified triangle-based pattern. The main factor in this model to adjust the bond strength is the attack angle and the height of the rib as well as the distance between two adjacent ribs.

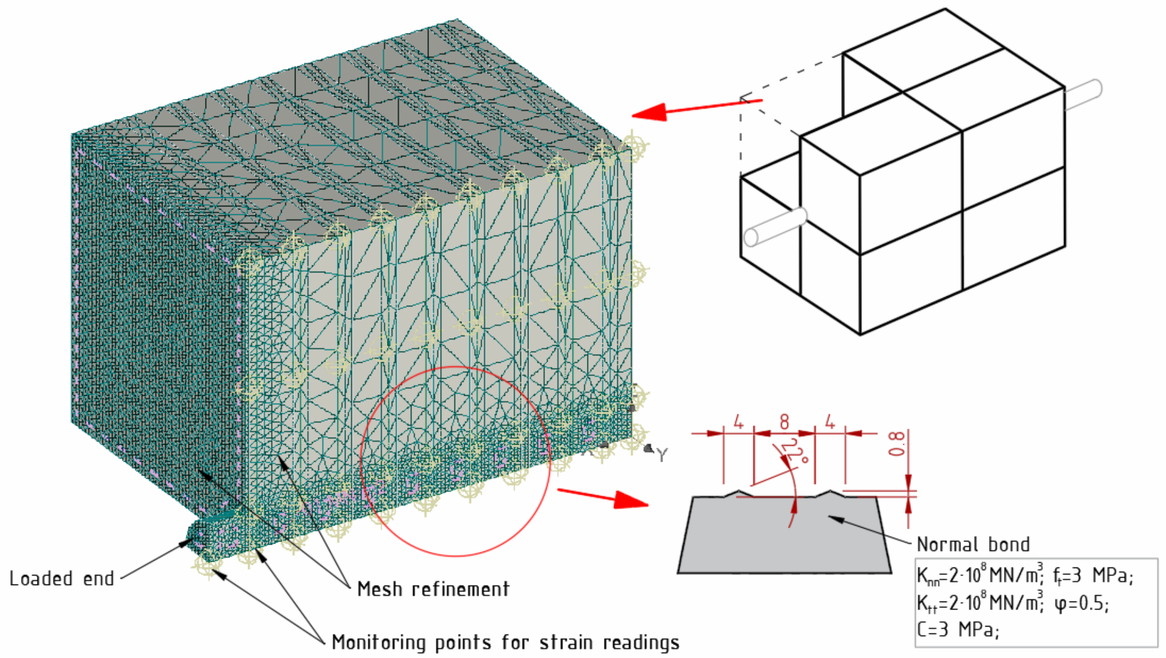

Figure 6. FE Model-2 with assumed bond characteristics

Similar to the previously discussed *Model-1*, this model is also made from isoparametric tetrahedral elements with 10 nodes. For the attack angle of the ribs is $\theta = 22°$ and the height of rib of 0.8 mm. Bonding index is the main parameter relating the simplified geometry used in FE analysis and the geometry of nominal rebars. For this particular configuration of the rib the calculated bonding index is 0.07 (Metelli & Plizzari, 2014). The distance between two adjacent ribs is 12 mm. "Normal" bond was adopted for all surfaces of interaction. Tensile load up to 90 kN was applied at 5kN steps based on the *Standard Newton-Raphson* parameters analysis. For simplicity, the loss of cross-sectional area was compensated by higher stresses in the reinforcement.

Strains in concrete at the maximum tensile load (90kN) are displayed in Figure 7. As the specimen was chosen intentionally to be shorter than the mean crack spacing, no transverse cracking is observed. The macro-cracking pattern itself is common and likely expected, thus giving encouragement that considered model is a highly effective one. It is interesting to observe cracking at the surface of concrete cover, what might be the initiation of splitting cracks (Figure 7b). The detailed observation of these analyses is further discussed in the next chapter.

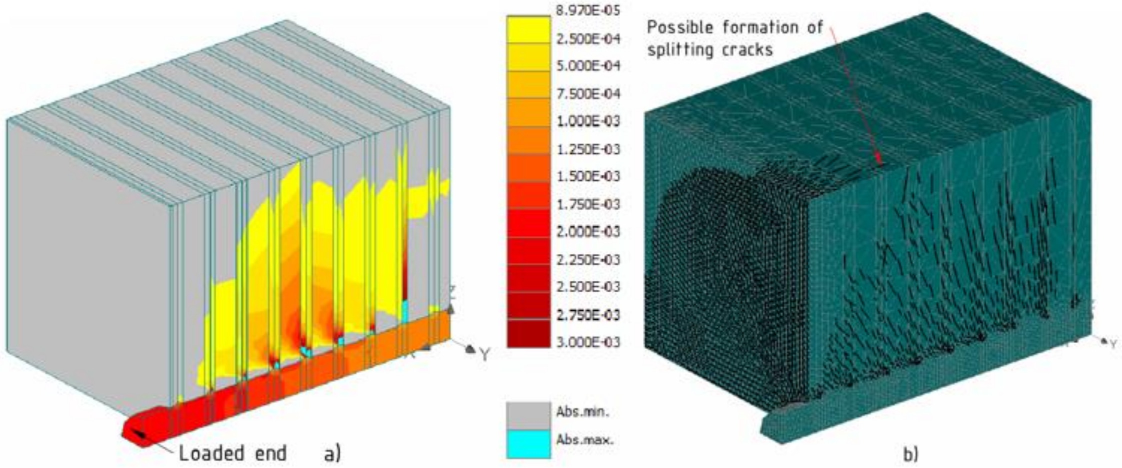

Figure 7. FE Model-2 (a) longitudinal concrete strain profile and (b) failure mechanics

4. Results and discussion

Figure 8 compares experimentally extracted reinforcement strain curves and the strain curves obtained from two different numerical FE models. The results of four load stages are presented in Figure 8.

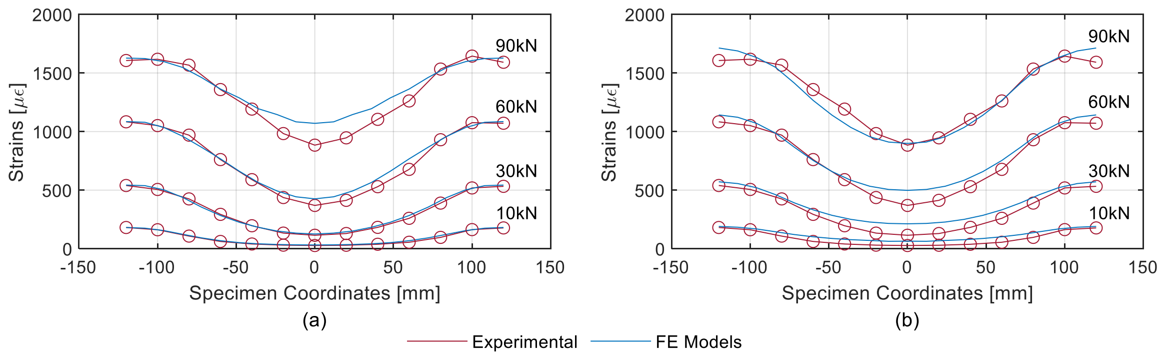

Figure 8. Experimental strain profile comparison with (a) FE Model-1 and (b) FE Model-2

Strain profile of both the finite element *Model-1* and *Model-2* were separately compared with the experimental counterpart in Figure 8a and 8b, respectively. The circular indications on the red (experimental) curves represent the location of strain gauge installed 20 mm apart. *Model-1* shows a very good correlation with experimental data at lower loads (Figure 8a). At higher loads, the steel strains obtained from *Model-1* tend to get flatten and more discrepancies from the test results the strain profiles are observed. Furthermore, the FE analysis failed to converge with the experimental outputs at higher loads. The reason for this might be the fundamental assumption in the *Model-1*, as it does not consider the radial component of bond stresses. A slight disparity is visible in the comparison of *Model-2* and experimental strains, particularly in the middle portion of the specimen (Figure 8b).

Further analysis of reinforcement strain data has been carried out on the basis of stress transfer approach. Obtained strain data was used to determine bond stress at every segment, $\tau(x)$ using the Equation (1).

$$\tau(x) = \frac{d\varepsilon(x)}{dx}\frac{E\emptyset}{4} \tag{1}$$

Where E is the modulus of elasticity of the reinforcement; $\emptyset$ is the bar diameter (20mm in our investigation); ε is the reinforcement strain. It is assumed that the subjected tensile load is distributed between the reinforcement as well as the surrounded concrete. Accordingly, the concrete strains were easily calculated from the reinforcement strains obtained from the experiments at different load stages. Fictitiously the specimens were divided in several small segments and slip was determined at each of the segments from the strain difference between the two materials. Following the same concept, step by step calculations were performed for the experimental and numerical models using MatLab programing. Some parts of the analysis were demonstrated through only the half-length of the specimen (Figure 9) using the symmetric property of the specimen along its longitudinal axis.

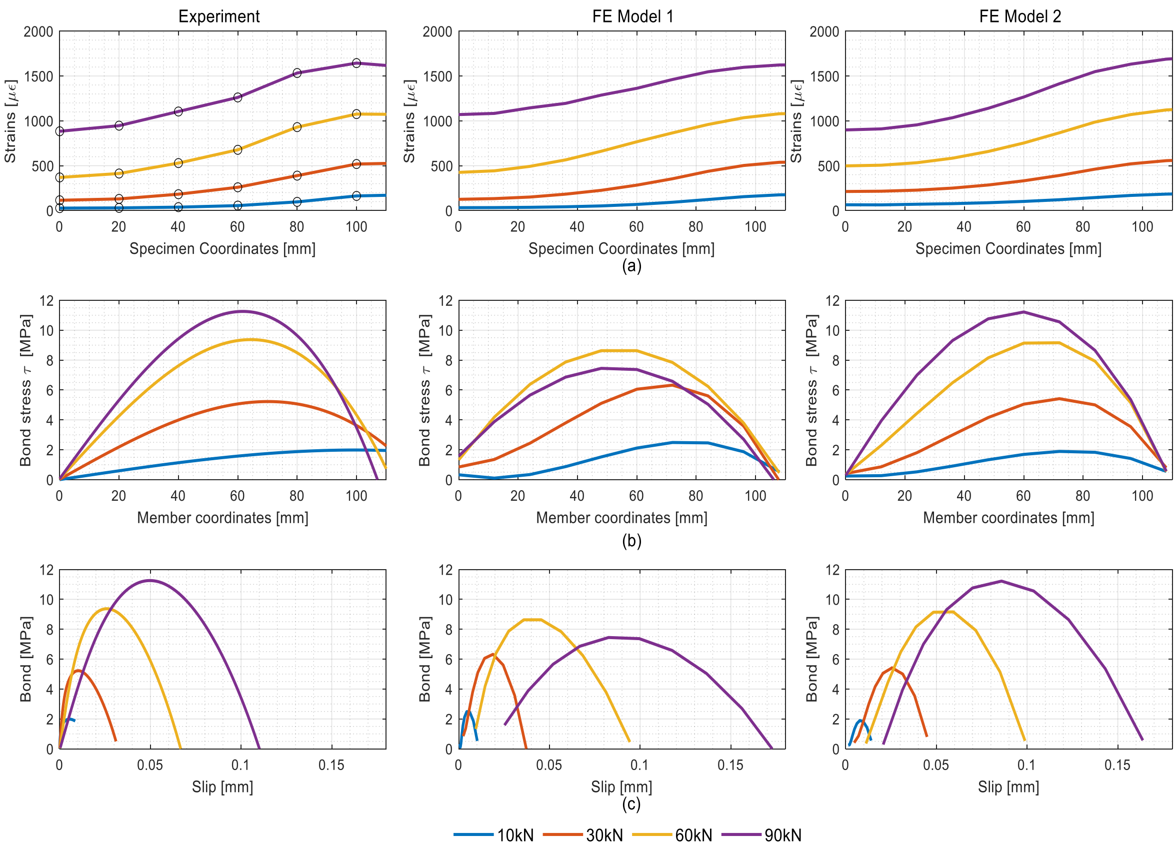

Figure 9. Result and analysis of experimental and FE Models (a) extracted strain profile (b) bond stress profile and (c) bond-slip relationship

Figure 9(a) displays the symmetrically half strain profile obtained from the experimental result and numerical modelling. The bond stress along the length of the specimen is shown in Figure 9(b) where it is clearly visible that the maximum bond stress obtained from the test at the maximum load stage (P=90kN) was 11.2 MPa. While the predictions by *Model-2* were close to this value, but *Model-1* resulted much lesser bond tress at the same load level (indicating the purple line in Figure 9b). This reduction in the bond stress at higher loads can be related to the absence of mechanical interlock (no rib condition) at the reinforcement-concrete interface. Alongside the no-rib system (*Model-1*) does not account the radial component of stresses and once the applied stress exceeds the shear and tensile capacity of the concrete, the bond deterioration begins, hence significant drop in bond stress has been noticed in the case of *Model-1* (Figure 9b).

Also the bond-slip relationship at the concrete-reinforcement interface at different load levels have been plotted, represented in Figure 9(c). At higher load stages, *Model-2* demonstrates good agreement with the experiment in terms of bond stresses and bond stress - slip diagrams (Figure 9c). The presence of three-dimensional ribs probably made *Model-2* more realistic. Though the agreement with the experiment was not so good at lower load levels, the predictions at higher loads representing the serviceability limit are more important in terms of cracking and bond behaviour. FE *Model-2* seems to be a promising instrument for prediction of cracking and deformation of a large-scale engineering problem. However, more experimental and numerical investigations are required to develop a more universal model which will be capable to accurately predict cracking and deformations in a more complex stress and strain state.

5. Conclusion

In this study, two different finite element approaches were introduced to investigate the three-dimensional stress-state of bond in the reinforced concrete ties subjected to tension. The soundness of numerical models were validated with the experimental data. Comparison of achieved results led to the following conclusions:

- FE *Model-1* approach demonstrated good correlation with experiments at low loading levels. Though, main drawback of the model is that it does not simulate transfer or radial stresses from reinforcement to the surrounding concrete. This shortcoming turns critical at the final loading levels, when shear strength of concrete was exceeded and failure of bonding was observed, thus compromising reliability and accuracy of considered model.
- FE *Model-2* approach showed a very good compliance with the extracted experimental data. It proved to be an effective instrument for investigation of RC elements behaviour and for prediction of longitudinal and transversal crack propagation. Of course, validity of model should also be verified with elements in bending. This could be the objective of future investigations.
- Both finite element models are noticeably sensitive to the levels of applied load. It might be important to further investigate the key parameters that affect the bond stress transfer mechanism and establish new qualified values for them.

Acknowledgements

The study was performed within the project that has received funding from European Social Fund (project No 09.3.3-LMT-K-712-01-0145) under grant agreement with the Research Council of Lithuania (LMTLT).

References

Balázs, G. L. (2007). Connecting Reinforcement to Concrete by Bond. *Beton- Und Stahlbetonbau*, *102*(S1), 46–50. https://doi.org/10.1002/best.200710109

Bernardi, P., Cerioni, R., Ferretti, D., & Michelini, E. (2014). Role of multiaxial state of stress on cracking of RC ties. *Engineering Fracture Mechanics*, *123*, 21–33. https://doi.org/10.1016/j.engfracmech.2014.02.011

Borosnyói, A., & Snóbli, I. (2010). Crack width variation within the concrete cover of reinforced concrete members. *Epitoanyag - Journal of Silicate Based and Composite Materials*, *62*(3), 70–74. https://doi.org/10.14382/epitoanyag-jsbcm.2010.14

Cervenka, V., Jendele, L., & Cervenka, J. (2007). ATENA Program Documentation Part 1 Theory. In *ATENA rogram documentation Part I theory. Cervenka Consulting, Prague* (p. 231).

Daoud, A., Maurel, O., & Laborderie, C. (2013). 2D mesoscopic modelling of bar – concrete bond. *Engineering Structures*, *49*, 696–706. https://doi.org/10.1016/j.engstruct.2012.11.018

Dey, A., Bado, M. F., Sokolov, A., & Kaklauskas, G. (2020). Distributed sensing, fiber bragg gratings and strain gauges for strain monitoring of rc tensile element. *Fib Symposium 2020, Concrete Structures for Resilient Society*, 2028–2035.

Dey, A., Vastrad, A. V., Bado, M. F., Sokolov, A., & Kaklauskas, G. (2021). Long-Term Concrete Shrinkage Influence on the Performance of Reinforced Concrete Structures. *Materials*, *14*(254), 1–16. https://doi.org/10.3390/ma14020254

fib Model Code, 2010. (2013). fib model code for concrete structures 2010. *International Federation for Structural*

Concrete(FIb), Switzerland, Federal Institute of Technology Lausanne-EPFI. http://repositorio.unan.edu.ni/2986/1/5624.pdf

Gambarova, P. G. (2012). Bond in Reinforcement Concrete: where do we stand today? *Bond in Concrete 2012-General Aspects of Bond*, 1–11.

Goto, Y. (1971). Cracks Formed in Concrete Around Deformed Tension Bars. *American Concrete Institute*, *68*(4), 244–251.

Jakubovskis, R., & Kaklauskas, G. (2019). Bond-stress and bar-strain profiles in RC tension members modelled via finite elements. *Engineering Structures*, *194*(January), 138–146. https://doi.org/10.1016/j.engstruct.2019.05.069

Jendele, L., & Cervenka, J. (2006). Finite element modelling of reinforcement with bond. *Computers & Structures*, *84*, 1780–1791. https://doi.org/10.1016/j.compstruc.2006.04.010

Kaklauskas, G. (2017). Crack Model for RC Members Based on Compatibility of Stress-Transfer and Mean-Strain Approaches. *Journal of Structural Engineering (United States)*, *143*(9), 1–12. https://doi.org/10.1061/(ASCE)ST.1943-541X.0001842

Kaklauskas, G., Ramanauskas, R., & Jakubovskis, R. (2017). Mean crack spacing modelling for RC tension elements. *Engineering Structures*, *150*, 843–851. https://doi.org/10.1016/j.engstruct.2017.07.090

Kaklauskas, G., Sokolov, A., Ramanauskas, R., & Jakubovskis, R. (2019). Reinforcement Strains in Reinforced Concrete Tensile Members Recorded by Strain Gauges and FBG Sensors : Experimental and Numerical Analysis. *Sensors*, *19*(200), 1–13. https://doi.org/10.3390/s19010200

Kanazawa, T., Sato, Y., & Mikawa, T. (2017). Modeling of Bond Deterioration between Steel Bar and Concrete Subjected to Freeze-thaw Action. *Journal of Advanced Concrete Technology*, *15*, 397–406. https://doi.org/10.3151/jact.15.397

Lutz, B. L. A., & Gergely, P. (1967). Mechanics of Bond and Slip of Deformed Bars in Concrete. *Aci Journal*, *64*, 711–721.

Metelli, G., & Plizzari, G. A. (2014). Influence of the relative rib area on bond behaviour. *Magazine of Concrete Research*, *66*(6), 277–294.

Ruiz, M. F., Muttoni, A., & Gambarova, P. G. (2007). Analytical modeling of the pre – and post – yield behavior of bond in reinforced concrete. *Journal of Structural Engineering*, *133*(10), 1364–1372.

Salem, H. M., & Maekawa, K. (2004). Pre- and Postyield Finite Element Method Simulation of Bond of Ribbed Reinforcing Bars. *Journal of Structural Engineering*, *130*(April), 671–680.

Santos, J., & Abel, A. (2015). New finite element to model bond – slip with steel strain effect for the analysis of reinforced concrete structures. *Engineering Structures*, *86*, 72–83. https://doi.org/10.1016/j.engstruct.2014.12.036

Shang, F., An, X., Mishima, T., & Maekawa, K. (2011). Three-dimensional Nonlinear Bond Model incorporating Transverse Action in Corroded RC Members. *Journal of Advanced Concrete Technology*, *9*(1), 89–102.

Siempu, R., & Pancharathi, R. K. (2018). A study on the parameters influencing flexural bond stress in reinforced concrete. *Structures*, *16*(September), 198–207. https://doi.org/10.1016/j.istruc.2018.09.006

Sulaiman, M. F., Ma, C. K., Apandi, N. M., Chin, S., Awang, A. Z., Mansur, S. A., & Omar, W. (2017). A Review on Bond and Anchorage of Confined High-strength Concrete. *Structures*, *11*(January), 97–109. https://doi.org/10.1016/j.istruc.2017.04.004